

Randomized Shortest Paths with Net Flows and Capacity Constraints

Draft manuscript subject to changes

Sylvain Courtain, Pierre Leleux, Ilkka Kivimaki,
Guillaume Guex & Marco Saerens

Abstract

This work extends the randomized shortest paths model (RSP) by investigating the net flow RSP and adding capacity constraints on edge flows. The standard RSP is a model of movement, or spread, through a network interpolating between a random walk and a shortest path behavior [44, 67, 80]. This framework assumes a unit flow injected into a source node and collected from a target node with flows minimizing the expected transportation cost together with a relative entropy regularization term. In this context, the present work first develops the net flow RSP model considering that edge flows in opposite directions neutralize each other (as in electrical networks) and proposes an algorithm for computing the expected routing costs between all pairs of nodes. This quantity is called the net flow RSP dissimilarity measure between nodes. Experimental comparisons on node clustering tasks show that the net flow RSP dissimilarity is competitive with other state-of-the-art techniques. In the second part of the paper, it is shown how to introduce capacity constraints on edge flows and a procedure solving this constrained problem by using Lagrangian duality is developed. These two extensions improve significantly the scope of applications of the RSP framework.

1 Introduction

Link analysis and network science are devoted to the analysis of network data and are currently studied in a large number of different fields (see, e.g., [5, 11, 16, 25, 27, 46, 49, 57, 68, 72, 77]). One recurring problem in this context is the definition of meaningful measures capturing interesting properties of the network and its nodes, like distance measures between nodes or centrality measures. These quantities usually take the structure of the whole network into account.

However, many such measures are based on some strong assumptions about the movement, or communication, in the network whose two extreme cases are the optimal behavior and the random behavior. Indeed, the two most popular distance measures in this context are the least-cost distance (also called shortest-path distance) and the resistance distance [45] (equal to the effective resistance and proportional to the commute-time distance when considering a random walk on the graph [26]). The same holds with the betweenness centrality; popular measures are the shortest path betweenness introduced by Freeman [30] (based on shortest paths) and the random-walk betweenness (also called the current-flow betweenness) introduced both by Newman [56] and

by Brandes and Fleischer [12], independently. Still another example is provided by the measures of compactness of a network, the Wiener index (based on shortest paths; see, e.g., [11]) and the Kirchhoff index (based on random walks or electrical networks; see, e.g., [45]).

However, in reality, behavior is seldom based on optimality or complete randomness. Therefore, in the last years, there has been a large effort invested in defining models interpolating between shortest-path and random-walk behaviors, especially in the context of defining distance measures between nodes taking both proximity and high connectivity into account [27]. Some of these models are based on extensions of electrical networks [3, 38, 58, 76], some on combinatorial analysis arguments [13, 14, 15], some on mixed L1-L2 regularization [50, 51], some on entropy-regularized network flow models [6, 36], and still others on entropy-regularized least-cost paths ([28, 44, 67, 80], inspired by a transportation model developed in [2] and related to [73]) – the **randomized shortest-path (RSP)** framework, which is the main subject of this paper. For a more thorough discussion of families of distances between nodes, see, e.g., [27, 28, 44].

Recently, the RSP has also been successfully used in, e.g., defining betweenness measures interpolating between a variant of the shortest-path betweenness and the random-walk betweenness [43], modelling the behavior of animals [61], and fraud detection [18].

This effort is pursued here by proposing two extensions of this model, considering

- ▶ a new dissimilarity measure extending the RSP dissimilarity [44, 67, 80], namely the **net-flow RSP dissimilarity**. This new dissimilarity is – like the standard RSP dissimilarity – the expected cost needed for reaching the target node from the source node, but now considering that edge flows in two opposite directions cancel out, as for electrical currents. An algorithm is proposed for computing the net-flow RSP dissimilarity matrix between all pairs of nodes.
- ▶ the introduction of **capacity constraints** in the model. Capacity constraints on edge flows are very common in practice [1, 23] and it would certainly increase significantly the applicability of the RSP model if such constraints could be integrated. Therefore, the main contributions related to capacity constraints are (1) to show how the model can accommodate such constraints, for both raw edge flows and net edge flows, and (2) to provide an algorithm for solving the constrained RSP model in the case of a single pair of source/target nodes.

The contents of the paper are as follows. Section 2 summarises the standard RSP framework. Section 3 introduces the net flow RSP dissimilarity. Then, Section 4 develops new algorithms for constraining the flow capacity on edges, while Section 5 deals with net flow capacity constraints. Illustrative examples and experiments on node clustering tasks are described in Section 6. Finally, Section 7 is the conclusion.

2 The standard randomized shortest path framework

As already discussed, the main contributions of the paper are based on the RSP framework, interpolating between a least-cost and a random-walk behavior, and allowing to define dissimilarity measures between nodes [67, 80, 44, 27]. The formalism is based on full paths instead of standard “local” edge flows [1, 23] and is briefly described in

this section for completeness. We start by providing a short account of the RSP formalism before introducing, in the next sections, the net flow RSP dissimilarity as well as the algorithm for solving the flow-capacity constrained problem on a directed graph.

2.1 Background and notation

Let us first introduce some necessary notation [27, 28]. First, notice that column vectors are written in bold lowercase and matrices are in bold uppercase.

In this work, we consider a weighted directed¹, strongly connected graph, $G = (\mathcal{V}, \mathcal{E})$, with a set \mathcal{V} of n nodes and a set \mathcal{E} of edges. An edge connecting node i to node j is denoted by (i, j) or $i \rightarrow j$.

Furthermore, we are given an adjacency matrix $\mathbf{A} = (a_{ij}) \geq 0$ quantifying the directed affinity between node i and node j . We further assume that there are no self-loops in the network, that is, $a_{ii} = 0$ for all i .

From this adjacency matrix, the standard **reference random walk** on the graph is defined in the usual way: the **transition probabilities** associated to each node are set proportionally to the affinities and then normalized in order to sum to one,

$$p_{ij}^{\text{ref}} = \frac{a_{ij}}{\sum_{j'=1}^n a_{ij'}} = \frac{a_{ij}}{d_i} \quad (1)$$

where d_i is the (out)degree of node i . The matrix $\mathbf{P}_{\text{ref}} = (p_{ij}^{\text{ref}})$ is stochastic and is called the transition matrix of the natural, reference, random walk on the network.

Furthermore, a transition **cost**, $c_{ij} \geq 0$, is associated to each edge (i, j) of the graph G . If there is no edge linking i to j , the cost is assumed to take an infinite value, $c_{ij} = \infty$. For consistency, we assume that $c_{ij} = \infty$ if $a_{ij} = 0$. The cost matrix is defined accordingly, $\mathbf{C} = (c_{ij})$.

A **path** or **walk** φ is a finite sequence of hops to adjacent nodes on G (including cycles), initiated from a starting node s and stopping in some ending, target, node t . A **hitting path** is a path where the last node t does not appear as an intermediate node. In other words, a hitting path to node t stops when it reaches t for the first time. We consider hitting paths to the fixed target node t by setting this target node as absorbing (or “killing”). Computationally this is achieved by setting the corresponding row t of the adjacency matrix and of the transition matrix to zero.

The node along path φ at position τ on the path is denoted by $\varphi(\tau)$. The **total cost** of a path, $\tilde{c}(\varphi)$, is simply the sum of the edge costs c_{ij} along φ while its **length** $\ell(\varphi)$ is the number of steps, or hops, needed for following that path. Costs are usually set independently of the adjacency matrix; they quantify the cost of a transition, depending on the application (see [28] for a discussion). In electrical networks, the costs are resistances and the affinities are conductances; in this context, they are linked by $a_{ij} = 1/c_{ij}$.

2.2 The standard randomized shortest path formalism

The main idea behind the RSP model is the following. Let us consider the set of all hitting paths, or walks, $\varphi \in \mathcal{P}_{st}$ from a node $s \in \mathcal{V}$ (source) to an absorbing, killing, node $t \in \mathcal{V}$ (target) on G . Each path φ consists in a sequence of connected nodes

¹If the graph is undirected, we consider that it is made of two, reciprocal, directed edges with the same affinities and costs.

starting in node s and ending in t . Then, we assign a probability distribution $P(\cdot)$ on the discrete set of paths \mathcal{P}_{st} by minimizing the free energy [6, 40, 44, 62, 65],

$$\begin{cases} \text{minimize} & \phi(P) = \sum_{\varphi \in \mathcal{P}_{st}} P(\varphi) \tilde{c}(\varphi) + T \sum_{\varphi \in \mathcal{P}_{st}} P(\varphi) \log \left(\frac{P(\varphi)}{\tilde{\pi}(\varphi)} \right) \\ \text{subject to} & \sum_{\varphi \in \mathcal{P}_{st}} P(\varphi) = 1 \end{cases} \quad (2)$$

where $\tilde{c}(\varphi) = \sum_{\tau=1}^{\ell(\varphi)} c_{\varphi(\tau-1)\varphi(\tau)}$ is the total cumulated cost along path φ when visiting the nodes $(\varphi(\tau))_{\tau=0}^{\ell(\varphi)}$ in the sequential order. Furthermore, $\tilde{\pi}(\varphi) = \prod_{\tau=1}^{\ell(\varphi)} p_{\varphi(\tau-1)\varphi(\tau)}^{\text{ref}}$ is the product of the reference transition probabilities along path φ , i.e., the random walk probability of path φ .

The objective function (Eq. 2) is a mixture of two dissimilarity terms, with the temperature $T > 0$ balancing the trade-off between them. The first term is the expected cost for reaching target node from source node (favoring shorter paths – *exploitation*). The second term corresponds to the relative entropy, or Kullback-Leibler divergence, between the path probability distribution and the reference path probability distribution (introducing randomness – *exploration*). For a low temperature T , shorter paths are favoured whereas when T is large, paths are chosen according to their likelihood in the reference random walk on the graph G . This argument, akin to maximum entropy [40, 42, 19], leads to a **Gibbs-Boltzmann distribution** on the set of paths (see, e.g., [28]),

$$P^*(\varphi) = \frac{\tilde{\pi}(\varphi) \exp[-\theta \tilde{c}(\varphi)]}{\sum_{\varphi' \in \mathcal{P}_{st}} \tilde{\pi}(\varphi') \exp[-\theta \tilde{c}(\varphi')]} = \frac{\tilde{\pi}(\varphi) \exp[-\theta \tilde{c}(\varphi)]}{\mathcal{Z}} \quad (3)$$

where $\theta = 1/T$ is the inverse temperature and the denominator $\mathcal{Z} = \sum_{\varphi \in \mathcal{P}_{st}} \tilde{\pi}(\varphi) \exp[-\theta \tilde{c}(\varphi)]$ is the **partition function** of the system.

It can be shown that, for intermediary temperatures T , this set of path probabilities is exactly equivalent to a Markov chain with biased transition probabilities favoring shorter paths [67].

Interestingly, if we replace the probability distribution $P(\cdot)$ by the optimal distribution $P^*(\cdot)$ provided by Eq. 3 in the objective function (Eq. 2), we obtain

$$\begin{aligned} \phi^* = \phi(P^*) &= \sum_{\varphi \in \mathcal{P}_{st}} P^*(\varphi) \tilde{c}(\varphi) + T \sum_{\varphi \in \mathcal{P}_{st}} P^*(\varphi) \log \left(\frac{P^*(\varphi)}{\tilde{\pi}(\varphi)} \right) \\ &= \sum_{\varphi \in \mathcal{P}_{st}} P^*(\varphi) \tilde{c}(\varphi) + T \sum_{\varphi \in \mathcal{P}_{st}} P^*(\varphi) \left(-\frac{1}{T} \tilde{c}(\varphi) - \log \mathcal{Z} \right) \\ &= -T \log \mathcal{Z} \end{aligned} \quad (4)$$

which is called the directed **free energy distance** [44]. It has been shown that when considering the continuous-time continuous-state limit, this quantity plays the role of a potential in a diffusion process [32].

2.3 Computing quantities of interest

Moreover quantities of interest can be computed by taking the partial derivative of the optimal free energy [27, 28, 44, 67, 80]. Here, we only introduce the quantities that are needed in order to derive the algorithms developed later.

Fundamental matrix It turns out that the partition function can be computed in closed form from an auxiliary matrix (see, e.g., [27, 43, 67]). Let us first introduce the **fundamental matrix** of the RSP system,

$$\mathbf{Z} = \mathbf{I} + \mathbf{W} + \mathbf{W}^2 + \dots = (\mathbf{I} - \mathbf{W})^{-1} \quad \text{with} \quad \mathbf{W} = \mathbf{P}_{\text{ref}} \circ \exp[-\theta \mathbf{C}] \quad (5)$$

where \mathbf{C} is the cost matrix and \circ is the elementwise (Hadamard) product. The equation sums up contributions of different paths lengths, starting from zero-length paths (identity matrix \mathbf{I}). Recall that the target node t is made killing and absorbing by setting the corresponding row of the reference transition matrix to zero, which implies that row t of \mathbf{W} is also zero.

Partition function and backward variables The partition function is then given by $\mathcal{Z} = [\mathbf{Z}]_{st} = z_{st}$ where s, t are the source and target nodes (see [80, 67, 44, 28]).

More generally, it can be shown that [31]

$$z_{it} = \sum_{\varphi \in \mathcal{P}_{it}} \tilde{\pi}(\varphi) \exp[-\theta \tilde{c}(\varphi)] \quad (6)$$

where \mathcal{P}_{it} is the set of hitting paths starting in node i and ending in node t . The z_{it} are usually called the backward variables. Note that these backward variables can be interpreted as probabilities of surviving during a killed random walk with transition matrix \mathbf{W} , that is, reaching hitting node t without being killed during the walk [28].

Computation of flows and numbers of visits The directed flow on edge (i, j) (the expected number of passages through (i, j) when going from s to t) can be obtained from Eq. 4 and Eq. 5 for a given temperature $T = 1/\theta$ (see [67, 43] for details) by

$$\bar{n}_{ij} \triangleq \sum_{\varphi \in \mathcal{P}_{st}} P(\varphi) \eta((i, j) \in \varphi) = -\frac{1}{\theta} \frac{\partial \log \mathcal{Z}}{\partial c_{ij}} = \frac{z_{si} w_{ij} z_{jt}}{z_{st}} \quad (7)$$

where $\eta((i, j) \in \varphi)$ counts the number of times edge (i, j) appears on path φ . Now, as only the first row and the last column of \mathbf{Z} are needed, two systems of linear equations can be solved instead of matrix inversion in Eq. 5. We further define the matrix containing the expected number of passages through edges (i, j) by $\mathbf{N} = (\bar{n}_{ij})$. From the last Eq. 7, the expected **number of visits** to a node j can also be defined, and easily computed, as

$$\bar{n}_j = \sum_{i \in \text{Pred}(j)} \bar{n}_{ij} + \delta_{sj} = \sum_{i=1}^n \bar{n}_{ij} + \delta_{sj} = \frac{z_{sj} z_{jt}}{z_{st}} + \delta_{sj}. \quad (8)$$

because a unit flow of $+1$ is injected in node s .

Optimal transition probabilities Finally, the optimal transition probabilities of following any edge (i, j) (the policy) induced by the set of paths \mathcal{P}_{st} and their probability mass (Eq. 3) are [67]

$$p_{ij}^* = \frac{\bar{n}_{ij}}{\sum_{j'=1}^n \bar{n}_{ij'}} = \frac{z_{jt}}{z_{it}} w_{ij} \quad \text{for all } i \neq t \quad (9)$$

which defines a **biased random walk** (a Markov chain) on G – the random walker is “attracted” by the target node t . The lower the temperature, the larger the attraction. Interestingly these transition probabilities do not depend on the source node and correspond to the optimal randomized strategy, or policy, for reaching target node, minimizing free energy (Eq. 2).

3 The net flow randomized shortest path dissimilarity

In this section, we introduce the **net flow RSP** dissimilarity extending the standard RSP dissimilarity developed in [44, 67, 80]. As for the standard RSP dissimilarity, it corresponds to the expected cost for reaching target node t from source node s but with the important difference that *net flows* are considered instead of raw flows. These measures are now introduced in this section.

3.1 Definition of the net edge flow

In some situations, for instance electrical networks [8, 24], only net flows matter. Intuitively, it means that the edge flows in opposite directions $i \rightarrow j$ and $j \rightarrow i$ compensate each other so that only the positive net flow, defined as $|\bar{n}_{ij} - \bar{n}_{ji}|$, is taken into account, where edge flows are defined in Eq. 7. Net flows have already been used in the RSP framework in order to define node betweenness measures [43], generalizing two previous models based on electrical currents [12, 56]. They are further investigated in this section in order to define a new dissimilarity measure between nodes of a graph.

As for electrical currents [8, 24], the non-negative net flow in each edge (i, j) , denoted here as j_{ij} , is given in the RSP formalism by

$$j_{ij} = \max((\bar{n}_{ij} - \bar{n}_{ji}), 0) \quad (10)$$

or, in matrix form,

$$\mathbf{J} = \max((\mathbf{N} - \mathbf{N}^T), \mathbf{0}) \quad (11)$$

where the maximum is taken elementwise. This means that, for each edge, the net flow is defined (that is, positive) in only one direction², and is equal to zero in the other direction.

Interestingly, because the flow is equal to zero in one of the two edge directions, the net flow defines a directed graph from the source to the destination node, even if the original graph is undirected.

In many situations, net flows look intuitively more natural because of the flow compensation mechanism common to electricity.

3.2 Expected net cost and net RSP dissimilarity measure

The **expected cost** until absorption by target node t at temperature T can easily be computed in closed form from the RSP formalism. This expected cost spread in the network has been used as a dissimilarity measure between nodes [44, 67, 80] and was

²Another common convention is to consider $j_{ij} = (\bar{n}_{ij} - \bar{n}_{ji})$, and thus $j_{ji} = -j_{ij}$.

called the directed **RSP dissimilarity**. More formally, in the standard RSP framework, the expected cost spread in the network [31] is given by

$$\langle \tilde{c} \rangle = \sum_{\varphi \in \mathcal{P}_{st}} P(\varphi) \tilde{c}(\varphi) \quad (12)$$

Let us now express the cost along path φ as $\tilde{c}(\varphi) = \sum_{(i,j) \in \mathcal{E}} \eta((i,j) \in \varphi) c_{ij}$ where we saw that $\eta((i,j) \in \varphi)$ is the number of times edge (i,j) appears on path φ and \mathcal{E} is the set of edges. Injecting this last result in Eq. 12 provides

$$\langle \tilde{c} \rangle = \sum_{(i,j) \in \mathcal{E}} \left(\underbrace{\sum_{\varphi \in \mathcal{P}_{st}} P(\varphi) \eta((i,j) \in \varphi)}_{\text{expected number of passages } \bar{n}_{ij}} \right) c_{ij} = \sum_{(i,j) \in \mathcal{E}} \bar{n}_{ij} c_{ij} \quad (13)$$

or, in matrix form,

$$\langle \tilde{c} \rangle = \mathbf{e}^T (\mathbf{N} \circ \mathbf{C}) \mathbf{e} \quad (14)$$

where \circ is the elementwise matrix product and \mathbf{N} is the matrix of expected number of passages through edges defined in Eq. 7. This quantity is just the cumulative sum of the expected number of passages through each edge times the cost of following the edge.

When dealing with net flows instead, the Eq. 13, now computing the expected *net cost*, becomes

$$\langle \tilde{c}_{\text{net}} \rangle = \mathbf{e}^T [\max((\mathbf{N} - \mathbf{N}^T), \mathbf{0}) \circ \mathbf{C}] \mathbf{e} = \mathbf{e}^T (\mathbf{J} \circ \mathbf{C}) \mathbf{e} \quad (15)$$

This quantity can be interpreted as the net cost needed to reach the target node t from the source node s in a biased random walk (defined by Eq. 3 or Eq. 9) attracting the walker toward the target node t . It is therefore the equivalent of the expected first passage cost defined in Markov chain theory [60, 71], translated in the RSP formalism and for net flows. It can be interpreted as a directed dissimilarity between the starting node s and the target node t taking both proximity and amount of connectivity between s and t into account.

Therefore, the **net flow RSP dissimilarity** (nRSP, the counterpart of the standard RSP dissimilarity [44, 67, 80]) between node s and node t is defined as the symmetrized quantity

$$\Delta_{st}^{\text{nRSP}} = \langle \tilde{c}_{\text{net}} \rangle_{st} + \langle \tilde{c}_{\text{net}} \rangle_{ts} \quad (16)$$

where the starting and ending node need now to be specified again. This is an equivalent of the symmetric commute-cost quantity appearing in Markov chains [26]. When the temperature is large, $T \rightarrow \infty$, the directed dissimilarity $\langle \tilde{c}_{\text{net}} \rangle_{st}$ reduces to the least-cost distance between s and t , while when $T \rightarrow 0^+$, it tends to the expected net cost for a random walker moving according to the reference random walk (and thus electrical current). This quantity is in fact equivalent to the so-called R_1 distance introduced in [58], i.e., the weighted-by-costs sum of the net flows.

Notice the difference between this quantity and the energy spread in an electrical network. Indeed, if the costs are viewed as resistances, then, in the context of a resistive network, the energy weights the costs by the *squared* net flows – instead of the simple net flows in Eq. 15 [8, 24].

3.3 Net flows define a directed acyclic graph

Let us now show that the RSP net flows to a fixed target node t define a directed acyclic graph (DAG) when the reference probabilities are defined by Eq. 1 on the weighted undirected graph G . This comes from the fact that the net flows provided by Eq. 10 can be considered as an electrical current generated from a new graph \hat{G}_t derived from G by redefining its edge weights. Moreover, it is well-known that electrical current defines a DAG because current always follows edges in the direction of decreasing potential (voltage). The potential therefore defines a topological ordering [17] of the nodes from higher potential to lower one.

More precisely, for a fixed target t , let us define the graph \hat{G}_t by considering the following weights on edges (i, j)

$$\hat{a}_{ij} \triangleq z_{it} w_{ij} z_{jt} d_i = z_{it} p_{ij}^{\text{ref}} \exp(-\theta c_{ij}) z_{jt} d_i = z_{it} a_{ij} \exp(-\theta c_{ij}) z_{jt} \quad (17)$$

which is symmetric when \mathbf{A} and \mathbf{C} are symmetric. The natural transition probabilities on this new graph are provided by Eq. 1 where we replace a_{ij} by \hat{a}_{ij} ,

$$\hat{p}_{ij} = \frac{\hat{a}_{ij}}{\sum_{j'=1}^n \hat{a}_{ij'}} = \frac{w_{ij} z_{jt}}{\sum_{j'=1}^n w_{ij'} z_{j't}} = \frac{z_{jt}}{z_{it}} w_{ij} \quad \text{for all } i \neq t \quad (18)$$

which, from Eq. 9, are exactly the optimal RSP transition probabilities. Note that we used the relation $z_{it} = \sum_{j'=1}^n w_{ij'} z_{j't} + \delta_{it}$, which can be easily derived from the definition of the fundamental matrix (Eq. 5) (see also, e.g., [27, 44, 67, 80]).

This shows that the net flows resulting from the optimal biased random walk provided by Eq. 9 are generated by a random walk on \hat{G}_t (a Markov chain). From the equivalence between random walks on an undirected graph and electrical current on \hat{G}_t [24], this current defines a DAG.

3.4 Computation of the net flow randomized shortest path dissimilarity

This subsection shows how the net flow RSP dissimilarity between all pairs of nodes (Eq. 16) can be computed in matrix form from previous work [43]. Unfortunately, the computation of the net flow RSP dissimilarities is more time-consuming than computing the standard RSP dissimilarities, where it suffices to perform a matrix inversion [44]. This is because before being able to compute the dissimilarities, we need to find the net flows, which involves a non-linear function (max). It is, however, still feasible for small-to medium-size networks. The time complexity was shown to be $\mathcal{O}(n^3 + mn^2)$ where m is the number of edges [43], or $\mathcal{O}(m n^2)$ overall because $m \geq n$ for an undirected, connected, graph.

The algorithm for computing the net flow RSP dissimilarity is detailed in Algorithm 1. It uses a trick introduced in [34] for calculating the net flow between all source-destinations s, t in a particular edge (i, j) without having to explicitly turn node t into a killing, absorbing, node. More specifically, the procedure is an adaptation of Algorithm 2 in [43] (following Eq. 12 in this work, providing net flows) to the case of an undirected graph and the computation of net flow dissimilarities, instead of betweenness centrality. It is also optimized in order to loop over (undirected) edges only once: on line 10, the contributions of the two directions of edge (i, j) (one is necessarily equal to 0 and the other is equal to $|\bar{n}_{ij} - \bar{n}_{ji}|$) are summed together.

Algorithm 1 Computing the net flow randomized shortest-path dissimilarity matrix.

Input:

- An undirected, connected, graph G containing n nodes.
- The $n \times n$ symmetric adjacency matrix \mathbf{A} associated to G , containing affinities.
- The $n \times n$ reference transition probabilities matrix \mathbf{P}_{ref} associated to G (usually, the transition probabilities associated to the natural random walk on the graph, $\mathbf{P}_{\text{ref}} = \mathbf{D}^{-1}\mathbf{A}$).
- The $n \times n$ symmetric cost matrix \mathbf{C} associated to G .
- The inverse temperature parameter $\theta > 0$.

Output:

- The $n \times n$ randomized shortest-path net flow dissimilarity matrix Δ defined on all source-destination pairs.
1. $\mathbf{W} \leftarrow \mathbf{P}_{\text{ref}} \circ \exp[-\theta\mathbf{C}]$ \triangleright elementwise exponential and multiplication \circ
 2. $\mathbf{Z} \leftarrow (\mathbf{I} - \mathbf{W})^{-1}$ \triangleright the fundamental matrix
 3. $\Delta \leftarrow \mathbf{0}$ \triangleright initialize net RSP flow dissimilarity matrix
 4. **for** $i = 1$ to n **do** \triangleright compute contribution of each node i
 5. $\mathbf{z}_i^c \leftarrow \text{col}_i(\mathbf{Z}), \mathbf{z}_i^r \leftarrow \text{row}_i(\mathbf{Z})$ \triangleright copy column i and row i of \mathbf{Z} transformed into a column vector
 6. **for** $j \in \mathcal{N}(i)$ with $j > i$ **do** \triangleright loop on neighboring nodes j , considering each (undirected) edge only once
 7. $\mathbf{z}_j^c \leftarrow \text{col}_j(\mathbf{Z}), \mathbf{z}_j^r \leftarrow \text{row}_j(\mathbf{Z})$ \triangleright copy column j and row j of \mathbf{Z} transformed into a column vector
 8. $\mathbf{N}_{ij} \leftarrow w_{ij} \left[(\mathbf{z}_i^c (\mathbf{z}_j^r)^T \div \mathbf{Z}) - \mathbf{e} \left((\mathbf{z}_i^c \circ \mathbf{z}_j^r) \div \text{diag}(\mathbf{Z}) \right)^T \right]$ \triangleright matrix of flow in edge $i \rightarrow j$
for all source-destinations (see [43], Eq. 17)
 9. $\mathbf{N}_{ji} \leftarrow w_{ji} \left[(\mathbf{z}_j^c (\mathbf{z}_i^r)^T \div \mathbf{Z}) - \mathbf{e} \left((\mathbf{z}_j^c \circ \mathbf{z}_i^r) \div \text{diag}(\mathbf{Z}) \right)^T \right]$ \triangleright matrix of flow in edge $j \rightarrow i$
for all source-destinations (see [43], Eq. 17)
 10. $\text{Net}_{ij} \leftarrow \text{abs}(\mathbf{N}_{ij} - \mathbf{N}_{ji})$ \triangleright net flow contribution from edge $i \leftrightarrow j$
 11. $\Delta \leftarrow \Delta + c_{ij} \text{Net}_{ij}$ \triangleright update dissimilarity matrix with the contribution of edge $i \leftrightarrow j$
 12. **end for**
 13. **end for**
 14. $\Delta \leftarrow \Delta + \Delta^T$ \triangleright the resulting net RSP dissimilarities matrix
 15. **return** Δ
-

4 Dealing with edge flow capacity constraints

In this section, an algorithm computing the optimal policy under capacity flow constraints on edges is derived. For convenience³, we assume a weighted, undirected, connected, network G with a single source node (node s) and one single target node (node t). An input flow is injected in node s and absorbed in node t , but the model can easily be generalized to multiple sources and multiple destinations. As before, it is assumed that the target node t is killing and absorbing, meaning that the transition probabilities $p_{tj}^{\text{ref}} = 0$ for all nodes j , including node t .

The idea now is to constrain the flow visiting some edges belonging to a set of constrained edges \mathcal{C} . The expected number of passages through those edges (see Eq. 7) is therefore forced to not exceed some predefined values,

$$\bar{n}_{ij} \leq \sigma_{ij} \quad \text{for edges } (i, j) \in \mathcal{C} \quad (19)$$

which ensures that these flows on edges in \mathcal{C} are limited by the capacity $\sigma_{ij} > 0$ and thus must remain in the interval $[0, \sigma_{ij}]$. In this section, we consider that, although the graph G is undirected, the capacity constraints can be directed and thus active in only one direction of an edge. Therefore, each undirected edge $i \leftrightarrow j$ of G possibly leads to

³The results can easily be extended to multiple inputs and outputs, as well as directed graphs.

two directed edges (i, j) and (j, i) in \mathcal{C} , with different capacity constraints. Thus the set of constrained edges \mathcal{C} contains directed edges, indicating the direction of the capacity constraint.

Moreover, we assume that the constraints are feasible⁴. The solution will minimize the free energy objective function (Eq. 2) while satisfying these inequality constraints.

4.1 The Lagrange function in case of capacity constraints

From standard nonlinear optimization theory [7, 20, 34, 55], the Lagrange function is

$$\begin{aligned}
\mathcal{L}(\mathbf{P}, \boldsymbol{\Lambda}) &= \sum_{\wp \in \mathcal{P}_{st}} P(\wp) \tilde{c}(\wp) + T \sum_{\wp \in \mathcal{P}_{st}} P(\wp) \log \left(\frac{P(\wp)}{\tilde{\pi}(\wp)} \right) + \mu \left(\sum_{\wp \in \mathcal{P}_{st}} P(\wp) - 1 \right) \\
&\quad + \sum_{(i,j) \in \mathcal{C}} \lambda_{ij} (\bar{n}_{ij} - \sigma_{ij}) \\
&= \underbrace{\sum_{\wp \in \mathcal{P}_{st}} P(\wp) \tilde{c}(\wp) + T \sum_{\wp \in \mathcal{P}_{st}} P(\wp) \log \left(\frac{P(\wp)}{\tilde{\pi}(\wp)} \right)}_{\text{free energy, } \phi(\mathbf{P})} + \mu \left(\sum_{\wp \in \mathcal{P}_{st}} P(\wp) - 1 \right) \\
&\quad + \sum_{(i,j) \in \mathcal{C}} \lambda_{ij} \left(\underbrace{\sum_{\wp \in \mathcal{P}_{st}} P(\wp) \eta((i, j) \in \wp)}_{\bar{n}_{ij} \text{ (Eq. 7)}} - \sigma_{ij} \right) \tag{20}
\end{aligned}$$

where there is a Lagrange parameter μ associated to the sum to one constrain and a Lagrange parameter associated to each constrained edge and these Lagrange parameters $\{\lambda_{ij}\}$, $(i, j) \in \mathcal{C}$, are all nonnegative in the case of inequality constraints. Note that the objective function to be minimized with respect to the discrete probabilities (which is similar to Eq. 2) is convex and the equality constraints are all linear. The Lagrange function in Eq. 20 can be rearranged as

$$\begin{aligned}
\mathcal{L}(\mathbf{P}, \boldsymbol{\Lambda}) &= \sum_{\wp \in \mathcal{P}_{st}} P(\wp) \left(\tilde{c}(\wp) + \underbrace{\sum_{(i,j) \in \mathcal{C}} \lambda_{ij} \eta((i, j) \in \wp)}_{\text{augmented cost } \tilde{c}'(\wp) \text{ cumulated on path } \wp} \right) \\
&\quad + T \sum_{\wp \in \mathcal{P}_{st}} P(\wp) \log \left(\frac{P(\wp)}{\tilde{\pi}(\wp)} \right) + \mu \left(\sum_{\wp \in \mathcal{P}_{st}} P(\wp) - 1 \right) - \sum_{(i,j) \in \mathcal{C}} \lambda_{ij} \sigma_{ij} \\
&= \sum_{\wp \in \mathcal{P}_{st}} P(\wp) \sum_{(i,j) \in \mathcal{E}} \eta((i, j) \in \wp) \underbrace{(c_{ij} + \delta((i, j) \in \mathcal{C}) \lambda_{ij})}_{\text{augmented costs } c'_{ij}} \\
&\quad + T \sum_{\wp \in \mathcal{P}_{st}} P(\wp) \log \left(\frac{P(\wp)}{\tilde{\pi}(\wp)} \right) + \mu \left(\sum_{\wp \in \mathcal{P}_{st}} P(\wp) - 1 \right) - \sum_{(i,j) \in \mathcal{C}} \lambda_{ij} \sigma_{ij} \\
&= \underbrace{\sum_{\wp \in \mathcal{P}_{st}} P(\wp) \tilde{c}'(\wp) + T \sum_{\wp \in \mathcal{P}_{st}} P(\wp) \log \left(\frac{P(\wp)}{\tilde{\pi}(\wp)} \right)}_{\text{free energy based on augmented costs, } \phi'(\mathbf{P})} + \mu \left(\sum_{\wp \in \mathcal{P}_{st}} P(\wp) - 1 \right) \\
&\quad - \sum_{(i,j) \in \mathcal{C}} \lambda_{ij} \sigma_{ij} \tag{21}
\end{aligned}$$

⁴If not, the duality gap in our algorithm will not converge to zero.

Algorithm 2 Randomized shortest paths with capacity constraints.

Input:

- A weighted undirected graph G containing n nodes. Node s will be the source node and node t the absorbing, killing, target node.
- The $n \times n$ reference transition matrix \mathbf{P}_{ref} of the natural random walk on G .
- The $n \times n$ cost matrix \mathbf{C} associated to G defining non-negative costs of transitions. An infinite cost is associated to missing links.
- The set of constrained edges \mathcal{C} .
- The set of non-negative capacities on flows, $\{\sigma_{ij}\}$, defined on the set of constrained edges, $(i, j) \in \mathcal{C}$.
- The inverse temperature parameter $\theta > 0$.
- The gradient ascent step $\alpha > 0$.

Output:

- The $n \times n$ randomized policy provided by the transition matrix \mathbf{P}^* , defining a biased random walk on G satisfying the constraints.
1. $\mathbf{\Lambda} \leftarrow \mathbf{0}$ ▷ initialize the $n \times n$ Lagrange parameters matrix
 2. $\mathbf{C}' \leftarrow \mathbf{C}$ ▷ initialize the augmented costs matrix
 3. Set row t of matrix \mathbf{P}_{ref} to $\mathbf{0}^T$ ▷ target node t is made absorbing and killing
 4. **repeat** ▷ main iteration loop
 5. $\mathbf{W} \leftarrow \mathbf{P}_{\text{ref}} \circ \exp[-\theta \mathbf{C}']$ ▷ update \mathbf{W} matrix (elementwise exponential and multiplication \circ)
 6. Solve $(\mathbf{I} - \mathbf{W})\mathbf{z}_t = \mathbf{e}_t$ ▷ backward variables (column t of the fundamental matrix \mathbf{Z}) with elements z_{it}
 7. Solve $(\mathbf{I} - \mathbf{W})^T \mathbf{z}_s = \mathbf{e}_s$ ▷ forward variables (row s of the fundamental matrix \mathbf{Z} viewed as a column vector) with elements z_{si}
 8. $\mathbf{N} \leftarrow \frac{\text{Diag}(\mathbf{z}_s) \mathbf{W} \text{Diag}(\mathbf{z}_t)}{z_{st}}$ ▷ compute the expected number of passages in each edge
 9. **for all** $(i, j) \in \mathcal{C}$ **do** ▷ gradient ascend: update all quantities associated to constrained edges
 10. $\lambda_{ij} \leftarrow \max(\lambda_{ij} + 2\alpha(\bar{n}_{ij} - \sigma_{ij}), 0)$ ▷ update Lagrange parameters
 11. $c'_{ij} \leftarrow c_{ij} + \lambda_{ij}$ ▷ update augmented costs
 12. **end for**
 13. **until** convergence
 14. $\mathbf{P}^* \leftarrow (\text{Diag}(\mathbf{z}_t))^{-1} \mathbf{W} \text{Diag}(\mathbf{z}_t)$ ▷ compute optimal policy
 15. **return** \mathbf{P}^*
-

where the symbol $\delta((i, j) \in \mathcal{C})$ is defined as 1 when edge $(i, j) \in \mathcal{C}$ and 0 otherwise. Note that we used Eq. 4 and $\tilde{c}(\varphi) = \sum_{(i,j) \in \mathcal{E}} \eta((i, j) \in \varphi) c_{ij}$ (Eq. 13) computing the total cost along path φ .

During this derivation, we observed that the costs c_{ij} can be redefined into *augmented* costs integrating the additional “virtual” costs needed for satisfying the constraints, and provided by the Lagrange parameters,

$$c'_{ij} = \begin{cases} c_{ij} + \lambda_{ij} & \text{when edge } (i, j) \in \mathcal{C} \\ c_{ij} & \text{otherwise} \end{cases} \quad (22)$$

and $\mathbf{C}' = (c'_{ij})$ will be the matrix containing these augmented costs. Thus the Lagrange parameters have an interpretation similar to the dual variables in linear programming; they represent the extra cost to pay associated to each edge in order to satisfy the constraints [7, 20, 34, 55, 74]. This is also common in many network flow problems [1, 23].

Let $\phi'(\mathbf{P})$ be the free energy obtained in Eq. 21 from these augmented costs (Eq. 22). We now turn to the problem of finding the Lagrange parameters λ_{ij} by exploiting Lagrangian duality.

4.2 Exploiting Lagrangian duality

In this subsection, we will take advantage of the fact that, in our formulation of the problem, the Lagrange dual function and its gradient are easy to compute. Indeed, as the objective function is convex and all the equality constraints are linear, it is well-known that there is only one global minimum and the duality gap is zero⁵ [7, 20, 34, 55]. The optimum is a saddle point of the Lagrange function and a common optimization procedure (often called the Arrow-Hurwicz-Uzawa algorithm [4]) consists in sequentially (i) solving the primal (finding the optimal probability distribution) while considering the Lagrange parameters as fixed and then (ii) maximizing the dual (which is concave) with respect to the Lagrange parameters, until convergence. This procedure converges because the dual function is concave – see the mentioned references.

In our context, by denoting the matrix of Lagrange parameters as Λ , this provides the following steps [34], which are iterated until convergence,

$$\begin{cases} \mathcal{L}(\Lambda) = \mathcal{L}(P^*(\Lambda), \Lambda) = \underset{\{P(\varphi)\}_{\varphi \in \mathcal{P}_{st}}}{\text{minimize}} \mathcal{L}(P, \Lambda) & \text{(compute the dual function)} \\ \Lambda^* = \underset{\Lambda}{\text{arg max}} \mathcal{L}(\Lambda) & \text{(maximize the dual function)} \\ \Lambda = \Lambda^* \end{cases} \quad (23)$$

and this is the procedure that will be followed, where the dual function will be maximized through a simple gradient ascent procedure.

Computing the dual function

For computing the dual function $\mathcal{L}(P^*(\Lambda), \Lambda)$ in Eq. 23, we first have to find the optimal probability distribution P^* in terms of the Lagrange parameters. We thus have to compute the minimum of Eq. 21 for a constant Λ . But this Lagrange function (Eq. 21) is identical to the Lagrange function associated to the standard RSP optimization problem (Eq. 2), except that the costs c_{ij} are replaced by the augmented costs c'_{ij} , and the introduction of the last additional term, which does not depend on the probability distribution $P(\cdot)$. Therefore, the probability distribution minimizing Eq. 21 is a Gibbs-Boltzmann distribution of the form of Eq. 3, but now depending on the augmented costs instead of the original costs.

Then, we replace the probability distribution $P(\cdot)$ in $\mathcal{L}(P, \Lambda)$ by the optimal Gibbs-Boltzmann distribution $P^*(\cdot)$ depending on the augmented costs and thus also on the Lagrange parameters. From the result of Eq. 4, the obtained dual function (Eq. 23) is

$$\mathcal{L}(\Lambda) = \mathcal{L}(P^*(\Lambda), \Lambda) = -T \log \mathcal{Z}' - \sum_{(i,j) \in \mathcal{C}} \lambda_{ij} \sigma_{ij} \quad (24)$$

In this equation, \mathcal{Z}' is the partition function computed from the augmented costs \mathcal{C} and thus depends on Λ . We now need to maximize this dual function in function of these Lagrange parameters.

Maximizing the dual function

Let us now compute the gradient of the dual function with respect to the non-negative λ_{ij} for edges $(i, j) \in \mathcal{C}$. This maximization of the dual function can be done, e.g., by

⁵Recall that we assume that the problem is feasible.

using the simple method developed by Rockafellar (see [66], Eqs. 10 and 12). From $-T \partial \log \mathcal{Z} / \partial c_{ij} = \bar{n}_{ij}$ (Eq. 7), the gradient of the dual Lagrange function (Eq. 24), for $(i, j) \in \mathcal{C}$, is simply $\partial \mathcal{L}(\boldsymbol{\Lambda}) / \partial \lambda_{ij} = \partial(-T \log \mathcal{Z}' - \sum_{(k,l) \in \mathcal{C}} \lambda_{kl} \sigma_{kl}) / \partial \lambda_{ij} = \bar{n}_{ij} - \sigma_{ij}$,

where we used the definition of the augmented costs in Eq. 22 as well as Eq. 7. It can be observed that we simply recover the expressions for the capacity constraints. This is actually a standard result when dealing with maximum entropy problems (see, e.g., [41, 42]).

Then, for computing the Lagrange parameters, we thus follow [66] who proposed the following gradient-based updating rule⁶

$$\lambda_{ij} \leftarrow \max(\lambda_{ij} + 2\alpha(\bar{n}_{ij} - \sigma_{ij}), 0) \text{ for all } (i, j) \in \mathcal{C} \quad (25)$$

which is guaranteed to converge in the concave case, as far as α is positive, is not too large and the problem is feasible [66]. The update is iterated until convergence. Of course, we could have used other, more sophisticated and more efficient, optimization techniques (see, e.g., [7, 10, 34, 59]), but this simple procedure worked well for all our tests on small to medium graphs. The parameter α had to be tuned manually for each different data set, but this did not create any difficulty.

4.3 The resulting algorithm

The resulting algorithm is presented in Algorithm 2. It computes the optimal policy (Eq. 9) minimizing the objective function (Eq. 2) while satisfying the inequality constraints (Eq. 19). This optimal policy guides the random walker to the target state with a trade-off between exploitation and exploration monitored by temperature parameter T . The different steps of the procedure are the following:

- ▶ Initialize the Lagrange parameters to 0 and the augmented costs to the original edge costs \mathbf{C} .
- ▶ Then, iterate the following steps until convergence:
 - The elements of the fundamental matrix are recomputed from the current augmented costs (Eq. 5).
 - The expected number of passages through each edge (edge flows) is computed (Eq. 7).
 - The Lagrange parameters and the augmented costs are updated (Eqs. 25, 22).
- ▶ Compute and return the optimal policy (transition probabilities) according to Eq. 9.

Because a system of n linear equations needs to be solved at each iteration, its complexity is of order $\mathcal{O}(kn^3)$, depending on the number of iterations k needed for convergence, which is unknown in advance.

⁶We adopt the same convention as [66] by using 2α for the gradient step, although the factor 2 is not necessary here.

5 Dealing with net flow capacity constraints

Let us now consider the case where the capacities $\sigma_{ij} > 0$ with $(i, j) \in \mathcal{C}$ are defined on *net flows* instead of raw flows. It is therefore assumed in this section that the original graph is undirected and that the adjacency matrix as well as the cost matrix are symmetric. In this situation (see Eq. 10 and its discussion), the constraints operate on the net flows instead of the raw flows,

$$j_{ij} = \max((\bar{n}_{ij} - \bar{n}_{ji}), 0) \leq \sigma_{ij},$$

$$\text{or both } \begin{cases} \bar{n}_{ij} - \bar{n}_{ji} \leq \sigma_{ij} \\ \bar{n}_{ji} - \bar{n}_{ij} \leq \sigma_{ij} \end{cases} \text{ for each edge } (i, j) \in \mathcal{C} \quad (26)$$

For net flows, we further consider that σ_{ji} is always defined when there exists a capacity constraint σ_{ij} and that $\sigma_{ji} = \sigma_{ij}$ (symmetry). Then, in this last equation, only one of the two net flows is positive so that the constraint only operates in this direction of the flow: the second constraint is automatically satisfied. However, we formulate the constraints in both directions since we do not know a priori which one is potentially active. To summarize, if the set of constraints nodes \mathcal{C} contains edge (i, j) , it also necessarily contains its reciprocal (j, i) (they come by pair) with the same capacity value, $\sigma_{ji} = \sigma_{ij}$. We now turn to the derivation of the Lagrange function and the algorithm.

5.1 The Lagrange function in case of net flow capacity constraints

The Lagrange function then becomes, after re-arranging the terms like in Eq. 21 and using $\bar{n}_{ij} = \sum_{\varphi \in \mathcal{P}_{st}} P(\varphi) \eta((i, j) \in \varphi)$,

$$\begin{aligned} \mathcal{L}(P, \Lambda) &= \sum_{\varphi \in \mathcal{P}_{st}} P(\varphi) \tilde{c}(\varphi) + T \sum_{\varphi \in \mathcal{P}_{st}} P(\varphi) \log\left(\frac{P(\varphi)}{\tilde{\pi}(\varphi)}\right) + \mu \left(\sum_{\varphi \in \mathcal{P}_{st}} P(\varphi) - 1 \right) \\ &\quad + \sum_{(i,j) \in \mathcal{C}} \lambda_{ij} [\bar{n}_{ij} - \bar{n}_{ji} - \sigma_{ij}] \\ &= \sum_{\varphi \in \mathcal{P}_{st}} P(\varphi) \left(\tilde{c}(\varphi) + \sum_{(i,j) \in \mathcal{C}} \lambda_{ij} (\eta((i, j) \in \varphi) - \eta((j, i) \in \varphi)) \right) \\ &\quad + T \sum_{\varphi \in \mathcal{P}_{st}} P(\varphi) \log\left(\frac{P(\varphi)}{\tilde{\pi}(\varphi)}\right) + \mu \left(\sum_{\varphi \in \mathcal{P}_{st}} P(\varphi) - 1 \right) - \sum_{(i,j) \in \mathcal{C}} \lambda_{ij} \sigma_{ij} \end{aligned}$$

Now, from the symmetry of edges (edges are present by pairs; for each $(i, j) \in \mathcal{C}$: $(j, i) \in \mathcal{C}$), we deduce $\sum_{(i,j) \in \mathcal{C}} \lambda_{ij} \eta((j, i) \in \varphi) = \sum_{(j,i) \in \mathcal{C}} \lambda_{ij} \eta((j, i) \in \varphi) = \sum_{(i,j) \in \mathcal{C}} \lambda_{ji} \eta((i, j) \in \varphi)$. Injecting this result in the previous equation

and proceeding in the same way as in Eq. 21 provides

$$\begin{aligned}
\mathcal{L}(\mathbf{P}, \boldsymbol{\Lambda}) &= \sum_{\wp \in \mathcal{P}_{st}} \mathbf{P}(\wp) \left(\underbrace{\tilde{c}(\wp) + \sum_{(i,j) \in \mathcal{C}} (\lambda_{ij} - \lambda_{ji}) \eta((i,j) \in \wp)}_{\text{augmented cost } \tilde{c}'(\wp) \text{ cumulated on path } \wp} \right) \\
&\quad + T \sum_{\wp \in \mathcal{P}_{st}} \mathbf{P}(\wp) \log \left(\frac{\mathbf{P}(\wp)}{\tilde{\pi}(\wp)} \right) + \mu \left(\sum_{\wp \in \mathcal{P}_{st}} \mathbf{P}(\wp) - 1 \right) - \sum_{(i,j) \in \mathcal{C}} \lambda_{ij} \sigma_{ij} \\
&= \sum_{\wp \in \mathcal{P}_{st}} \mathbf{P}(\wp) \sum_{(i,j) \in \mathcal{E}} \eta((i,j) \in \wp) \underbrace{(c_{ij} + \delta((i,j) \in \mathcal{C}) (\lambda_{ij} - \lambda_{ji}))}_{\text{augmented costs } c'_{ij}} \\
&\quad + T \sum_{\wp \in \mathcal{P}_{st}} \mathbf{P}(\wp) \log \left(\frac{\mathbf{P}(\wp)}{\tilde{\pi}(\wp)} \right) + \mu \left(\sum_{\wp \in \mathcal{P}_{st}} \mathbf{P}(\wp) - 1 \right) - \sum_{(i,j) \in \mathcal{C}} \lambda_{ij} \sigma_{ij} \\
&= \underbrace{\sum_{\wp \in \mathcal{P}_{st}} \mathbf{P}(\wp) \tilde{c}'(\wp) + T \sum_{\wp \in \mathcal{P}_{st}} \mathbf{P}(\wp) \log \left(\frac{\mathbf{P}(\wp)}{\tilde{\pi}(\wp)} \right) + \mu \left(\sum_{\wp \in \mathcal{P}_{st}} \mathbf{P}(\wp) - 1 \right)}_{\text{free energy based on augmented costs, } \phi'(\mathbf{P})} \\
&\quad - \sum_{(i,j) \in \mathcal{C}} \lambda_{ij} \sigma_{ij} \tag{27}
\end{aligned}$$

which has exactly the same form as in the raw flow case (see Eq. 21) – only the definition of the augmented costs differs in the two expressions. Indeed, as before, the costs c_{ij} can be redefined into *augmented costs*,

$$c'_{ij} = \begin{cases} c_{ij} + \lambda_{ij} - \lambda_{ji} & \text{when edge } (i,j) \in \mathcal{C} \\ c_{ij} & \text{otherwise} \end{cases} \tag{28}$$

We must stress that we require that the constraints in Eq. 26 are symmetric and come by pairs.

By following the same reasoning as in the previous section (see Eq. 24 and 25), it can immediately be observed that the dual function has the same form and is provided by Eq. 24.

5.2 The resulting algorithm

Then, the gradient of the dual Lagrange function (Eq. 27) with augmented costs provided by Eq. 28 is $\partial \mathcal{L}(\boldsymbol{\Lambda}) / \partial \lambda_{ij} = \partial (-T \log \mathcal{Z}' - \sum_{(k,l) \in \mathcal{C}} \lambda_{kl} \sigma_{kl}) / \partial \lambda_{ij} = \bar{n}_{ij} - \bar{n}_{ji} - \sigma_{ij}$.

From this last result, we can derive the update of the Lagrange parameters in the net flow constraints case,

$$\lambda_{ij} \leftarrow \max(\lambda_{ij} + 2\alpha(\bar{n}_{ij} - \bar{n}_{ji} - \sigma_{ij}), 0) \text{ for all } (i,j) \in \mathcal{C} \tag{29}$$

The Algorithm 2 is easy to adapt in order to consider net flow capacity constraints: only lines 10 and 11 must be modified according to Eq. 29 and 28. Note also that constraints on net flows are defined for undirected graphs, the capacities being assumed to be symmetric.

6 Experiments

In this section, we first present two illustrative examples of the use of capacity constraints on the edge flows of a graph. Then, we evaluate the net flow RSP on unsupervised classification tasks and compare its results to other state-of-the-art graph node distances. We have to stress that our goal here is not to propose new node clustering algorithms outperforming state-of-the-art techniques. Rather, the aim is to investigate if the net flow RSP model is able to capture the community structure of networks in an accurate way, compared to other recent dissimilarity measures between nodes.

6.1 Illustrative examples

First example The first example illustrates the expected number of visits to nodes (see Eq. 8) over the RSP paths distribution between one source node s and one target node t on a 20×20 grid, in two different situations obtained after running the Algorithm 2. Nodes are linked to their neighbors⁷ with a unit affinity and a unit cost. In the first situation, we do not set any capacity constraint and the expected number of visits is represented in Fig. 1(a). As expected, it follows a trajectory close to the diagonal of the grid, representing the shortest paths between the source node and the target node.

In the second situation, we placed two obstacles (walls) by constraining the capacities of all the edges linking the nodes represented in red in Fig. 1(b) to 0.01. As can be observed in 1(c), this time, the expected number of visits to nodes no longer concentrates around the diagonal, but follows as close as possible the obstacles. This trajectory represents the least-cost paths between the source node and the target node avoiding the low-capacity obstacles.

Second example Our second illustrative example is taken from [63] and makes the link between the RSP with net flow capacity constraints and the maximum flow problem. Its aim is to show that the Algorithm 2 can be used to compute the maximum flow (which takes a value of 12 in this example) between the source node s and the target node t in the undirected graph G presented in Fig. 2. Each edge of this graph has a unit cost and affinity. Note that, in practice, because the RSP model assumes a unit input flow, all capacities are scaled⁸ so that the value of the maximum flow after scaling lies between 0 and 1. The maximum flow of G is then obtained by the reverse transformation.

To this end, we add a directed edge from s to t with infinite capacity and an edge cost of 10 to the original graph. This new edge introduces a “shortcut” edge allowing the passage of all the overflow of the graph, at the price of a higher cost. Theoretically, our algorithm will avoid going through this shortcut as much as possible because it has a high cost compared to the other edges in the graph. Therefore, it will try to maximize the flow that travels through the original network before using this shortcut edge.

Fig. 3 shows the evolution of the flow between the nodes $\{f, g, h\}$ and t (the flow through the original graph), provided by Algorithm 2, and thus satisfying the capacity constraints, in function of the value of the θ parameter. As observed in Fig. 3, this flow through the original network reaches almost exactly the maximum flow value of 12 for all θ larger than 1. However, when θ is low (close to zero), the flows become more and

⁷Only horizontal and vertical neighbors are considered (no diagonal edge).

⁸We divide by a graph cut, for instance the cut between nodes $\{f, g, h\}$ and t , 22 in our example.

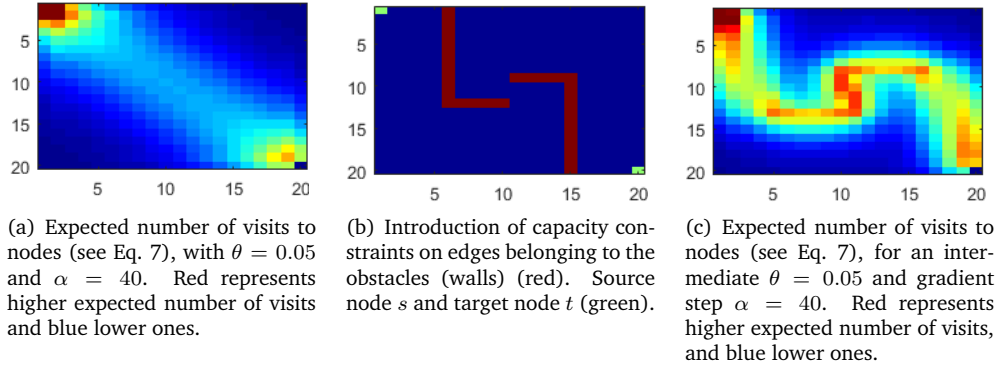


Figure 1: Illustrative example on a 2D grid.

more random, without considering costs any more (see Eq. 2). For that reason, part of the total flow goes through the shortcut, even if this is not optimal in terms of expected cost. This explains the reduction of the flow through the original network when θ is close to zero.

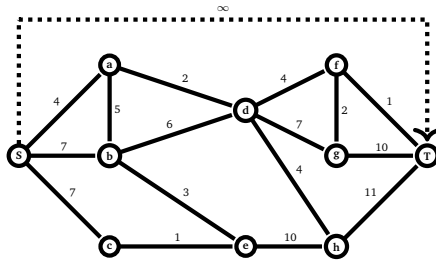


Figure 2: A small undirected graph composed of 8 nodes [63]. The values on the edges represent capacities; moreover all edge costs are set to 1, except the added shortcut edge whose cost is 10. The maximum flow between the source node s and the target node t is 12, and is equal to the min-cut between nodes $\{a, b, c\}$ and $\{d, e\}$.

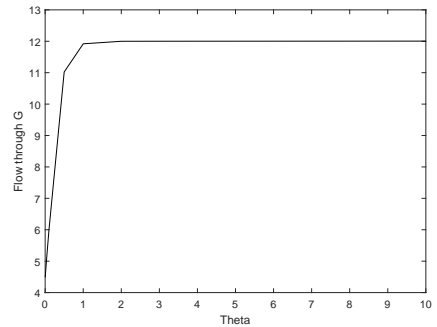


Figure 3: Evolution of the flow between nodes $\{f, g, h\}$ and t satisfying the capacity constraints (total flow in the original network G , without the shortcut edge), provided by Algorithm 2, in function of the $\theta = 1/T$ parameter, with a gradient step $\alpha = 1/\theta$. The intersection between the curve and the y -axis when $\theta \rightarrow 0^+$ is 4.467. Note that the x -axis is scaled logarithmically

6.2 Nodes clustering experiments

In this subsection, we present an application of the **Net Flow Randomized Shortest Paths** (nRSP)

in a graph nodes clustering context. Note that a methodology very close to [69] is used – see this paper for details.

Experimental Setup

Baseline dissimilarities As part of the node clustering experiment, four dissimilarity matrices between nodes will be used as baselines to assess our method.

- ▶ The **Free Energy** distance (FE) and the **Randomized Shortest Paths Dissimilarity** (RSP). Already presented earlier, these methods have been shown to perform well in a node clustering context [69] as well as in semi-supervised classification tasks [28].
- ▶ The **Corrected Commute Time** distance (CCT). The corrected commute time is an extension of the commute-time distance proposed in [75] in order to avoid the lost-in-space problem.
- ▶ The **Shortest Path** distance (SP). The distance corresponds to the cost along the shortest path between two nodes i and j , derived from the cost matrix C .

These dissimilarity matrices obtained by the different methods are then fed into a kernel k -means algorithm, after transforming the dissimilarities into inner products by multidimensional scaling (see later).

Datasets A collection of 17 datasets is investigated for the experimental comparisons of the dissimilarity measures. The collection includes Zachary’s karate club [81], the Dolphin datasets [52, 53], the Football dataset [33], the Political books⁹, three LFR benchmarks [47] and 9 Newsgroup datasets [48, 79]. The list of datasets along with their main characteristics are presented in Table 1.

Dataset Name	Clusters	Nodes	Edges
Dolphin_2	2	62	159
Dolphin_4	4	62	159
Football	12	115	613
LFR1	3	600	6142
LFR2	6	600	4807
LFR3	6	600	5233
Newsgroup_2.1	2	400	33854
Newsgroup_2.2	2	398	21480
Newsgroup_2.3	2	399	36527
Newsgroup_3.1	3	600	70591
Newsgroup_3.2	3	598	68201
Newsgroup_3.3	3	595	64169
Newsgroup_5.1	5	998	176962
Newsgroup_5.2	5	999	164452
Newsgroup_5.3	5	997	155618
Political books	3	105	441
Zachary	2	34	78

Table 1: Datasets used in our experiments.

Evaluation metrics Each partition provided by an investigated clustering technique will be assessed by comparing it with the “observed partition” of the dataset. Two criteria will be used to evaluate the similarity between both partitions.

⁹Collected by V. Krebs and labelled by M. Newman, this dataset is not published, but available for download at <http://www-personal.umich.edu/~mejn/netdata/>

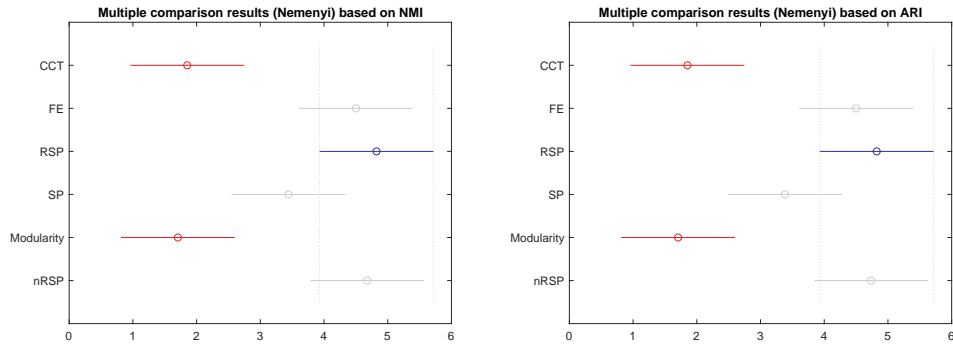


Figure 4: Mean ranks and 95% Nemenyi confidence intervals across the 17 datasets.

- ▶ The **Normalized Mutual Information (NMI)** [29, 70] between two partitions \mathcal{U} and \mathcal{V} is computed by dividing the mutual information [19] between the two partitions by the average of the respective entropy of \mathcal{U} and \mathcal{V} . See also [54].
- ▶ The **Adjusted Rand Index (ARI)** [39] is an extension of the Rand Index (RI) [64], which measures the degree of matching between two partitions. The RI presents the drawback of not showing a constant expected value when working with random partitions. On the contrary, the ARI has an expected value of 0 and a maximum value of 1.

Experimental methodology

The experimental methodology is similar to the one used in [69]. For each given dataset, the dissimilarity matrix \mathbf{D} obtained by the different methods is transformed into a kernel \mathbf{K} (a inner product matrix) using multidimensional scaling [9]. If the resulting kernel is not positive semi-definite, we simply set the negative eigenvalues to zero when computing the kernel.

As a second step, a kernel k -means (see e.g. [27, 79]) is run 30 times (trials) on \mathbf{K} . The NMI and ARI are computed for the partition minimizing the within-cluster inertia¹⁰ among the 30 trials. This second step is repeated 30 times (leading to a total of 900 runs of the k -means) to obtain the average within-cluster inertia, NMI and ARI scores for a given method (dissimilarity matrix) with a given value of its parameter (θ in the case of methods based on RSP) on a specific dataset.

The average within-cluster inertia (which is unsupervised) is used as a metrics to tune the parameter θ for the nRSP, the FE and the RSP (the lower, the better). The values tested for the parameter θ are $\{0.001, 0.005, 0.01, 0.05, 0.1, 0.5, 1, 3, 5, 10, 15, 20\}$.

Experimental results

The different methods are assessed globally using the same method as in [69] based on a non-parametric Friedman-Nemenyi test [22]. Additionally, a Wilcoxon signed-rank

¹⁰In this paper, the term “within-cluster inertia” refers to the within-cluster inertia divided by the total inertia, to obtain a value ranging from 0 to 1.

test [78] is performed pairwise to measure the significance of the difference in the algorithms performance.

In addition, the **Modularity matrix** \mathbf{Q} is used as last baseline (Modularity). The matrix is computed by $\mathbf{Q} = \mathbf{A} - \frac{\mathbf{d}\mathbf{d}^T}{\text{vol}}$ where \mathbf{d} contains the node degrees and the constant vol is the volume of the graph (see e.g. [27, 57]). The only difference with the other baselines is that the kernel k -means is executed directly on matrix \mathbf{Q} without using multidimensional scaling.

The results are summarized in Fig. 4. We can observe that both the Net Flow RSP, the FE and the RSP perform better than the CCT, the SP and the modularity matrix \mathbf{Q} . Although the differences between the SP and the FE, RSP and nRSP are not significant according to the Nemenyi test, when performing a Wilcoxon signed-rank test these differences happen to be significant at a $\alpha = 0.05$ level.

The introduced method obtains results comparable to the RSP and the FE for both measures based on the ARI and NMI. None of these differences are significant after performing a Wilcoxon signed rank test ($\alpha = 0.05$). Thus, the introduced nRSP method proves to be competitive with respect to the FE and the RSP which, in turn, performed best in a similar but more extensive node clustering comparison [69]. It can also be observed that the nRSP and the standard RSP obtain very similar performances, which was expected because both distances are based on the same framework.

7 Conclusion

In this work, we developed two extensions of the randomized shortest paths (RSP) formalism. The first extension introduces an algorithm for computing the expected net costs between all pairs of node, by considering the *net flows* between nodes instead of the raw flows. This quantity is called the net flow RSP dissimilarity; it quantifies the level of accessibility between nodes and serves as a dissimilarity measure. The second contribution shows how to deal with capacity constraints on edges for both raw and net flows in the RSP formalism. An algorithm solving the constrained problem is developed.

As already discussed in [37], the originality of the RSP model, in comparison with competing methods, lies in the fact that it adopts a *path-based formalism* with path relative entropy regularization; that is, the quantities of interest are defined on the set of all possible paths (or walks) between two nodes of the network. Another interesting feature is that most quantities of interest can be computed in closed form by using standard matrix operations.

These contributions extend significantly the scope of the RSP formalism, which basically defines a model of movement, or spread, through the network. Indeed, most of the traditional models are based on two common paradigms about the transfer of information, or more generally the movement, occurring in the network: an optimal behavior based on shortest paths and a random behavior based on a random walk on the graph.

Contrarily to these standard models, the RSP interpolates between a pure random walk on the graph and an optimal behavior based on shortest paths [28, 44, 67]. It depends on a temperature parameter allowing to monitor the amount of randomness of the trajectories. When the temperature is high, communication occurs through a random walk while, for low temperatures (close to zero), shorter paths are promoted. This acknowledges the fact that in many practical cases the (random) walker on the graph is neither completely rational, nor completely stochastic.

Experimental comparisons on clustering tasks showed that the net flow RSP is competitive in comparison with other state-the-art baseline methods. This shows that the model is able to capture the cluster structure of networks in an accurate way.

In conclusion, the contributions of this paper should enlarge significantly the range of possible applications of the RSP formalism. Indeed, many problems related to the spread of information in a network involve capacity constraints on edges. Moreover, in many real cases, it can be argued that a model based on unidirectional net flows is more realistic than raw flows going back and forth.

Concerning further work, we are interested in applications of the proposed models to operations research problems. For instance, it has been shown that solving optimal transport problems with entropic regularization can be significantly more efficient than using standard linear programming methods in some situations [21, 35, 37]. It would therefore be interesting to compare the RSP solution (with relative entropy regularization) to minimum-cost flow problems with capacity constraints to more standard algorithms [1, 23].

Acknowledgements

This work was partially supported by the Immediate and the Brufence projects funded by InnovIris (Brussels Region), as well as former projects funded by the Walloon region, Belgium. We thank these institutions for giving us the opportunity to conduct both fundamental and applied research.

References

- [1] R. K. Ahuja, T. L. Magnanti, and J. B. Orlin. *Network flows: Theory, algorithms, and applications*. Prentice Hall, 1993.
- [2] T. Akamatsu. Cyclic flows, Markov process and stochastic traffic assignment. *Transportation Research B*, 30(5):369–386, 1996.
- [3] M. Alamgir and U. von Luxburg. Phase transition in the family of p-resistances. In *Advances in Neural Information Processing Systems 24: Proceedings of the NIPS 2011 conference*, pages 379–387. MIT Press, 2011.
- [4] K. Arrow, L. Hurwicz, and H. Uzawa. *Studies in linear and non-linear programming*. Stanford University Press, 1958.
- [5] A. L. Barabasi. *Network science*. Cambridge University Press, 2016.
- [6] F. Bavaud and G. Guex. Interpolating between random walks and shortest paths: A path functional approach. In K. Aberer, A. Flache, W. Jager, L. Liu, J. Tang, and C. Guéret, editors, *Proceedings of the 4th International Conference on Social Informatics (SocInfo '12)*, volume 7710 of *Lecture Notes in Computer Science*, pages 68–81. Springer, 2012.
- [7] D. P. Bertsekas. *Nonlinear programming*. Athena Scientific, 2nd edition, 1999.

- [8] B. Bollobas. *Modern graph theory*. Springer, 2nd edition, 1998.
- [9] I. Borg and P. Groenen. *Modern multidimensional scaling: Theory and applications*. Springer, 1997.
- [10] S. Boyd and L. Vandenberghe. *Convex optimization*. Cambridge University Press, 2004.
- [11] U. Brandes and T. Erlebach, editors. *Network analysis: Methodological foundations*. Springer, 2005.
- [12] U. Brandes and D. Fleischer. Centrality measures based on current flow. In *Proceedings of the 22nd Annual Symposium on Theoretical Aspects of Computer Science (STACS '05)*, pages 533–544, 2005.
- [13] P. Chebotarev. A class of graph-geodetic distances generalizing the shortest-path and the resistance distances. *Discrete Applied Mathematics*, 159(5):295–302, 2011.
- [14] P. Chebotarev. The walk distances in graphs. *Discrete Applied Mathematics*, 160(10–11):1484–1500, 2012.
- [15] P. Chebotarev. Studying new classes of graph metrics. In F. Nielsen and F. Barbaresco, editors, *Proceedings of the 1st International Conference on Geometric Science of Information (GSI '13)*, volume 8085 of *Lecture Notes in Computer Science*, pages 207–214. Springer, 2013.
- [16] F. Chung and L. Lu. *Complex graphs and networks*. American Mathematical Society, 2006.
- [17] T. Cormen, C. Leiserson, R. Rivest, and C. Stein. *Introduction to algorithms*. MIT Press, 3rd edition, 2009.
- [18] S. Courtain, B. Lebichot, I. Kivimäki, and M. Saerens. Graph-based fraud detection with the free energy distance. In *Paper submitted for publication*, 2019.
- [19] T. M. Cover and J. A. Thomas. *Elements of information theory*. Wiley, 2nd edition, 2006.
- [20] J. Culioli. *Introduction a l'optimisation*. Ellipses, 2012.
- [21] M. Cuturi. Sinkhorn distances: lightspeed computation of optimal transport. In *Advances in Neural Information Processing Systems 26: Proceedings of the NIPS '13 conference*, pages 2292–2300. MIT Press, 2013.
- [22] J. Demšar. Statistical comparisons of classifiers over multiple data sets. *Journal of Machine learning research*, 7(Jan):1–30, 2006.
- [23] A. Dolan and J. Aldous. *Networks and algorithms: An introductory approach*. Wiley, 1993.
- [24] P. G. Doyle and J. L. Snell. *Random walks and electric networks*. The Mathematical Association of America, 1984.
- [25] E. Estrada. *The structure of complex networks*. Oxford University Press, 2012.

- [26] F. Fouss, A. Pirotte, J.-M. Renders, and M. Saerens. Random-walk computation of similarities between nodes of a graph, with application to collaborative recommendation. *IEEE Transactions on Knowledge and Data Engineering*, 19(3):355–369, 2007.
- [27] F. Fouss, M. Saerens, and M. Shimbo. *Algorithms and models for network data and link analysis*. Cambridge University Press, 2016.
- [28] K. Francoise, I. Kivimäki, A. Mantrach, F. Rossi, and M. Saerens. A bag-of-paths framework for network data analysis. *Neural Networks*, 90:90–111, 2017.
- [29] A. L. Fred and A. K. Jain. Robust data clustering. In *2003 IEEE Computer Society Conference on Computer Vision and Pattern Recognition, 2003. Proceedings.*, volume 2, pages II–II. IEEE, 2003.
- [30] L. C. Freeman. A set of measures of centrality based on betweenness. *Sociometry*, 40(1):35–41, 1977.
- [31] S. García-Díez, F. Fouss, M. Shimbo, and M. Saerens. A sum-over-paths extension of edit distances accounting for all sequence alignments. *Pattern Recognition*, 44(6):1172–1182, 2011.
- [32] S. García-Díez, E. Vandebussche, and M. Saerens. A continuous-state version of discrete randomized shortest-paths. In *Proceedings of the 50th IEEE International Conference on Decision and Control (CDC '11)*, pages 6570–6577, 2011.
- [33] M. Girvan and M. E. J. Newman. Community structure in social and biological networks. *Proceedings of the National Academy of Sciences of the USA*, 99(12):7821–7826, 2002.
- [34] I. Griva, S. Nash, and A. Sofer. *Linear and nonlinear optimization*. SIAM, 2nd edition, 2008.
- [35] G. Guex. Interpolating between random walks and optimal transportation routes: Flow with multiple sources and targets. *Physica A: Statistical Mechanics and its Applications*, 450:264–277, 2016.
- [36] G. Guex and F. Bavaud. Flow-based dissimilarities: shortest path, commute time, max-flow and free energy. In B. Lausen, S. Krolak-Schwerdt, and M. Bohmer, editors, *Data science, learning by latent structures, and knowledge discovery*, volume 1564 of *Studies in Classification, Data Analysis, and Knowledge Organization*, pages 101–111. Springer, 2015.
- [37] G. Guex, I. Kivimäki, and M. Saerens. Randomized optimal transport on a graph: framework and new distance measures. *Network Science*, 7(1):88–122, 2019.
- [38] M. Herbster and G. Lever. Predicting the labelling of a graph via minimum p-seminorm interpolation. In *Proceedings of the 22nd Conference on Learning Theory (COLT '09)*, pages 18–21, 2009.
- [39] L. Hubert and P. Arabie. Comparing partitions. *Journal of classification*, 2(1):193–218, 1985.
- [40] E. T. Jaynes. Information theory and statistical mechanics. *Physical Review*, 106:620–630, 1957.

- [41] T. Jebara. *Machine learning: discriminative and generative*. Springer Science & Business Media, 2004.
- [42] J. N. Kapur. *Maximum-entropy models in science and engineering*. Wiley, 1989.
- [43] I. Kivimäki, B. Lebichot, J. Saramäki, and M. Saerens. Two betweenness centrality measures based on randomized shortest paths. *Scientific Reports*, 6:srep19668, 2016.
- [44] I. Kivimäki, M. Shimbo, and M. Saerens. Developments in the theory of randomized shortest paths with a comparison of graph node distances. *Physica A: Statistical Mechanics and its Applications*, 393:600–616, 2014.
- [45] D. J. Klein and M. Randić. Resistance distance. *Journal of Mathematical Chemistry*, 12(1):81–95, 1993.
- [46] E. D. Kolaczyk. *Statistical analysis of network data: Methods and models*. Springer Series in Statistics. Springer, 2009.
- [47] A. Lancichinetti, S. Fortunato, and F. Radicchi. Benchmark graphs for testing community detection algorithms. *Physical review E*, 78(4):046110, 2008.
- [48] K. Lang. Newsweeder: Learning to filter netnews. In *Machine Learning Proceedings 1995*, pages 331–339. Elsevier, 1995.
- [49] T. Lewis. *Network science*. Wiley, 2009.
- [50] Y. Li, Z.-L. Zhang, and D. Boley. The routing continuum from shortest-path to all-path: A unifying theory. In *Proceedings of the 31st International Conference on Distributed Computing Systems (ICDCS '11)*, pages 847–856. IEEE Computer Society, 2011.
- [51] Y. Li, Z.-L. Zhang, and D. Boley. From shortest-path to all-path: The routing continuum theory and its applications. *IEEE Transactions on Parallel and Distributed Systems*, 25(7):1745–1755, 2013.
- [52] D. Lusseau. The emergent properties of a dolphin social network. *Proceedings of the Royal Society of London. Series B: Biological Sciences*, 270(suppl.2):S186–S188, 2003.
- [53] D. Lusseau, K. Schneider, O. J. Boisseau, P. Haase, E. Slooten, and S. M. Dawson. The bottlenose dolphin community of doubtful sound features a large proportion of long-lasting associations. *Behavioral Ecology and Sociobiology*, 54(4):396–405, 2003.
- [54] C. Manning, P. Raghavan, and H. Schütze. *Introduction to information retrieval*. Cambridge University Press, 2008.
- [55] M. Minoux. *Programmation mathématique, 2nd ed.* Lavoisier, 2008.
- [56] M. E. J. Newman. A measure of betweenness centrality based on random walks. *Social Networks*, 27(1):39–54, 2005.
- [57] M. E. J. Newman. *Networks: An introduction*. Oxford University Press, 2010.

- [58] C. Ngyen and H. Mamitsuka. New resistance distances with global information on large graphs. In *Proceedings of the 19th International Conference on Artificial Intelligence and Statistics (AISTATS '16)*, pages 639–647, 2016.
- [59] J. Nocedal and S. Wright. *Numerical optimization*. Springer, 2nd edition, 2006.
- [60] J. R. Norris. *Markov chains*. Cambridge University Press, 1997.
- [61] M. Panzacchi, B. Van Moorter, O. Strand, M. Saerens, I. Kivimäki, C. St Clair, I. Herfindal, and L. Boitani. Predicting the continuum between corridors and barriers to animal movements using step selection functions and randomized shortest paths. *Journal of Animal Ecology*, 85(1):32–42, 2016.
- [62] L. Peliti. *Statistical mechanics in a nutshell*. Princeton University Press, 2011.
- [63] W. L. Price. *Graphs and networks: an introduction*. London Butterworths, 1971.
- [64] W. M. Rand. Objective criteria for the evaluation of clustering methods. *Journal of the American Statistical association*, 66(336):846–850, 1971.
- [65] L. E. Reichl. *A modern course in statistical physics*. Wiley, 2nd edition, 1998.
- [66] R. Rockafellar. The multiplier method of Hestenes and Powell applied to convex programming. *Journal of Optimization Theory and Applications*, 12(6):555–562, 1973.
- [67] M. Saerens, Y. Achbany, F. Fouss, and L. Yen. Randomized shortest-path problems: Two related models. *Neural Computation*, 21(8):2363–2404, 2009.
- [68] T. Silva and L. Zhao. *Machine learning in complex networks*. Springer, 2016.
- [69] F. Sommer, F. Fouss, and M. Saerens. Comparison of graph node distances on clustering tasks. *Artificial Neural Networks and Machine Learning Proceedings of ICANN 2016. Lecture Notes in Computer Science*, 9886:192–201, 2016. Springer.
- [70] A. Strehl and J. Ghosh. Cluster ensembles—a knowledge reuse framework for combining multiple partitions. *Journal of machine learning research*, 3(Dec):583–617, 2002.
- [71] H. M. Taylor and S. Karlin. *An introduction to stochastic modeling*. Academic Press, 3rd edition, 1998.
- [72] M. Thelwall. *Link analysis: An information science approach*. Elsevier, 2004.
- [73] E. Todorov. Linearly-solvable Markov decision problems. In *Advances in Neural Information Processing Systems 19 (NIPS 2006)*, pages 1369–1375. MIT Press, 2007.
- [74] S. Vajda. *Mathematical programming*. Addison-Wesley, 1961.
- [75] U. von Luxburg, A. Radl, and M. Hein. Getting lost in space: Large sample analysis of the commute distance. In *Advances in Neural Information Processing Systems 23: Proceedings of the NIPS '10 Conference*, pages 2622–2630, 2010.
- [76] U. von Luxburg, A. Radl, and M. Hein. Hitting and commute times in large random neighborhood graphs. *Journal of Machine Learning Research*, 15(1):1751–1798, 2014.

- [77] S. Wasserman and K. Faust. *Social network analysis: Methods and applications*. Cambridge University Press, 1994.
- [78] F. Wilcoxon. Individual comparisons by ranking methods. In *Breakthroughs in statistics*, pages 196–202. Springer, 1992.
- [79] L. Yen, F. Fouss, C. Decaestecker, P. Francq, and M. Saerens. Graph nodes clustering with the sigmoid commute-time kernel: A comparative study. *Data & Knowledge Engineering*, 68(3):338–361, 2009.
- [80] L. Yen, A. Mantrach, M. Shimbo, and M. Saerens. A family of dissimilarity measures between nodes generalizing both the shortest-path and the commute-time distances. In *Proceedings of the 14th ACM SIGKDD International Conference on Knowledge Discovery and Data Mining (KDD '08)*, pages 785–793, 2008.
- [81] W. W. Zachary. An information flow model for conflict and fission in small groups. *Journal of Anthropological Research*, 33(4):452–473, 1977.
-